Enhancing Constraints on First-Order Phase Transitions in the Early Universe Through Multi-Source Gravitational-Wave Background Analysis

K. O'Neal-Ault

August 28, 2025

Work in collaboration with J. Kersten and L. Velasco-Sevilla

Motivation

We are developing parameter estimation tools using Bayesian inference to:

- Characterize the SGWB generated by first-order phase transitions (FOPT) in the early Universe
- Disentangle cosmological signals from those of astrophysical origin
- Extend analyses beyond LVK detector sensitivities, e.g., to LISA, ET, DECIGO, etc. , etc.

Investigating FOPT sources from the early Universe requires:

- Analysis methods tailored for stochastic gravitational wave signals
- A clear strategy for modeling the sources of the stochastic gravitational wave background (SGWB)

Stochastic GW Signals

The stochastic gravitational wave background (SGWB) arises from a large number of weak, independent, and unresolved GW sources.

The properties of the radiation depend on the underlying sources.

Since individual signals cannot be resolved, the SGWB can only be characterized statistically.

Standard Assumptions:

- Isotropic
- Unpolarized
- Stationary
- Gaussian

The **likelihood function**:

$$p(\hat{C}_{ij}(f)|\theta) \propto exp\left[-\frac{1}{2}\sum_{ij}\sum_{f}\left(\frac{\hat{C}_{ij}(f)-\Omega_{GW}(f|\theta)}{\sigma_{ij}(f)}\right)^2\right] \quad (1)$$

Astrophysical Sources

Astrophysical sources discussed in the literature that may contribute to the SGWB include:

- Compact Binary Coalescences (CBCs)
- Neutron Stars (NSs)
- Supernovae
- The first stars

SGWB signals are described by:

$$\Omega_{GW}(f) = \frac{1}{\rho_c} \frac{d\rho_{GW}}{d \ln f}, \tag{2}$$

where $\rho_c = \frac{3c^2 H_0^2}{8\pi G}$ is the critical energy density of the Universe required to close it today.

CBC: Power Law

A simple power-law is often used to describe the dominant inspiral phase of CBC sources.

$$\Omega_{GW}(f) = A\left(\frac{f}{f_{\text{ref}}}\right)^{\alpha} \tag{3}$$

- A is the amplitude (only free parameter).
- f is measured in the detector frame and depends on detector sensitivity.
- In the adiabatic inspiral phase, the leading-order quadrupole approximation gives $\alpha = 2/3$[a],[b].

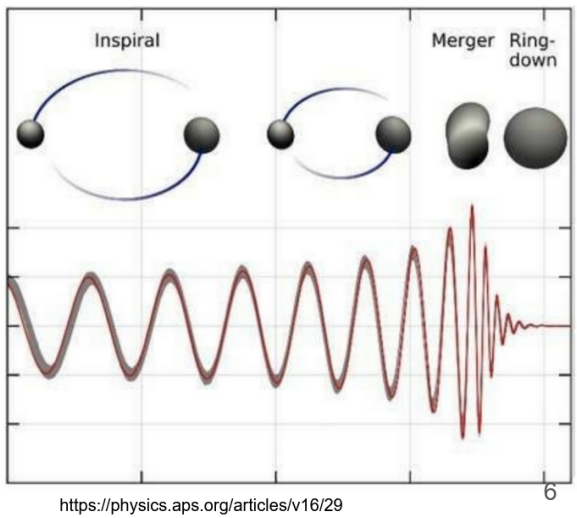

https://physics.aps.org/articles/v16/29

[a] B.P. Abbott et al., Phys. Rev. Lett., 116:131102, 2016

[b] C. Wu et al., Phys. Rev. D., 85:104024, 2012

CBC: Fiducial Expression

A more general fiducial form:

$$\Omega_{GW}(f) = \frac{f}{\rho_c H_0} \int_0^{z_{\max}} dz \, \frac{R(z) \, \frac{dE_{GW}}{df}}{(1+z) \, E_z(\Omega_M, \Omega_\Lambda, z)} \tag{4}$$

- $E_z(\Omega_M, \Omega_\Lambda, z) = \sqrt{\Omega_\Lambda + \Omega_M (1+z)^3}$ encodes the cosmological redshift dependence in a flat, ΛCDM Universe ($\Omega_\Lambda \sim 0.7$, $\Omega_M \sim 0.3$).
- $R(z)$ is the merger rate per comoving volume, determined by the cosmic star formation rate (CSFR) and the delay time between binary formation and coalescence.
- $\frac{dE_{GW}}{df}$ is the source spectral energy density. For LVK sensitivities, the inspiral phase dominates with scaling $\Omega_{GW} \propto M_c^{5/3} f^{2/3}$.

An example BNS system shown over 20–256 Hz, computed using (4)[1].

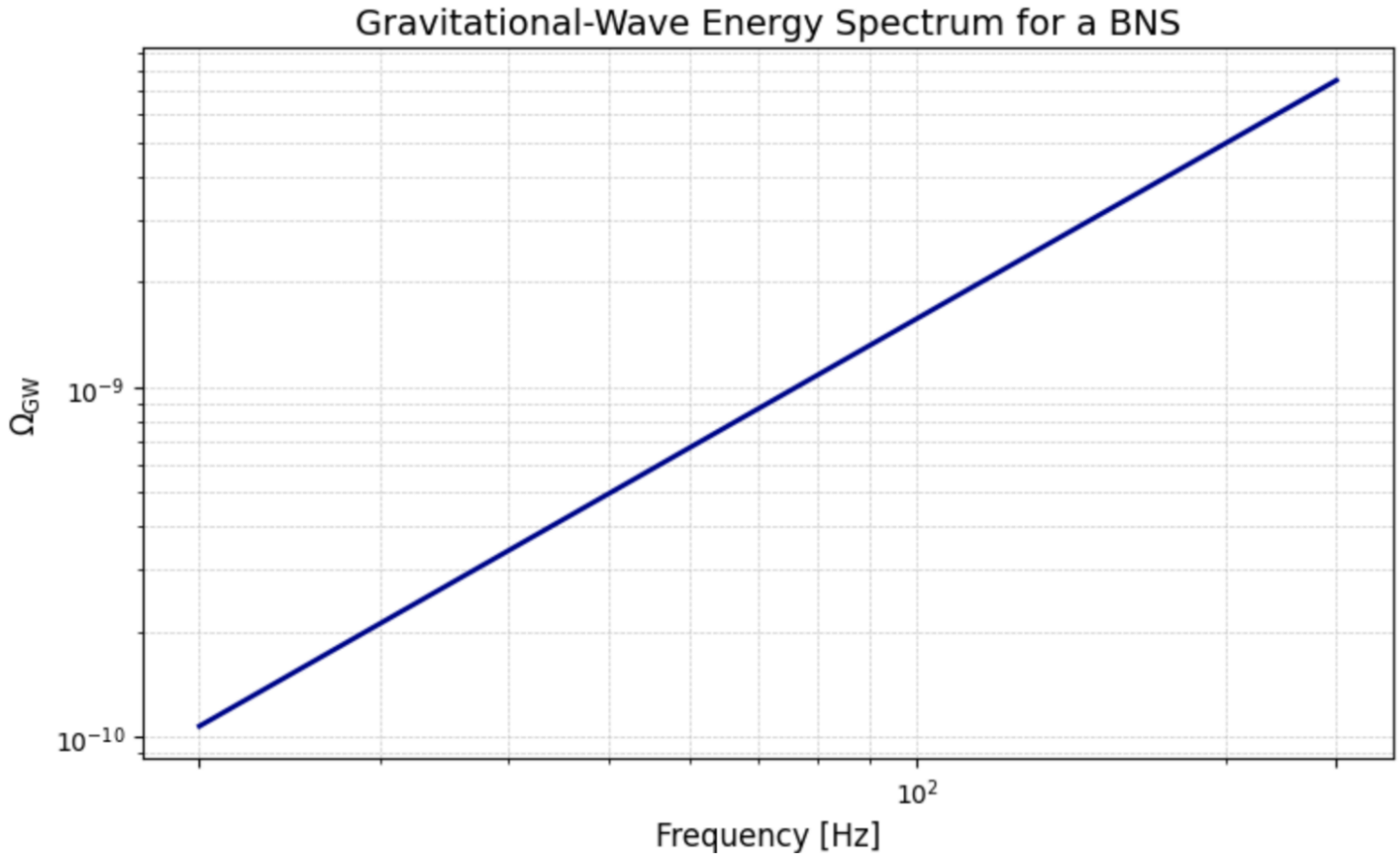

[1] C. Wu et al., Phys. Rev. D., 85:104024, 2012

Rotating Neutron Stars

Rotating NSs, including pulsars and magnetars, can contribute to the SGWB.[2],[3] For example, when the properties of the Galactic population are similar to those observed in pulsars we have:

$$\Omega_{GW}(f) = \frac{f}{c\rho_c} \int_0^{z_{\max}} dz \, \frac{1}{4\pi d_L(z)^2} \frac{dE_{GW}}{df} \frac{df_{\text{source}}}{df} \frac{dR(z)}{dz}. \quad (5)$$

- d_L is the luminosity distance.
- The spectral energy $\frac{dE_{GW}}{df}$ is model dependent.
- The event rate $\frac{dR(z)}{dz}$ is model dependent and includes the mass fraction of progenitors and the CSFR.

[2] T. Regimbau, V. Mandic, Class. Quant. Grav., 25:184018, 2008

[3] P. A. Rosado, Phys. Rev. D., 86:104007, 2012

To achieve a good fit between the predicted cosmic star formation rate (CSFR) and observations—using UV, Hα, far-infrared, and radio luminosities—a reddening correction is applied that varies with the CSFR[4],[5]. The redshift range is up to $z = 6$.

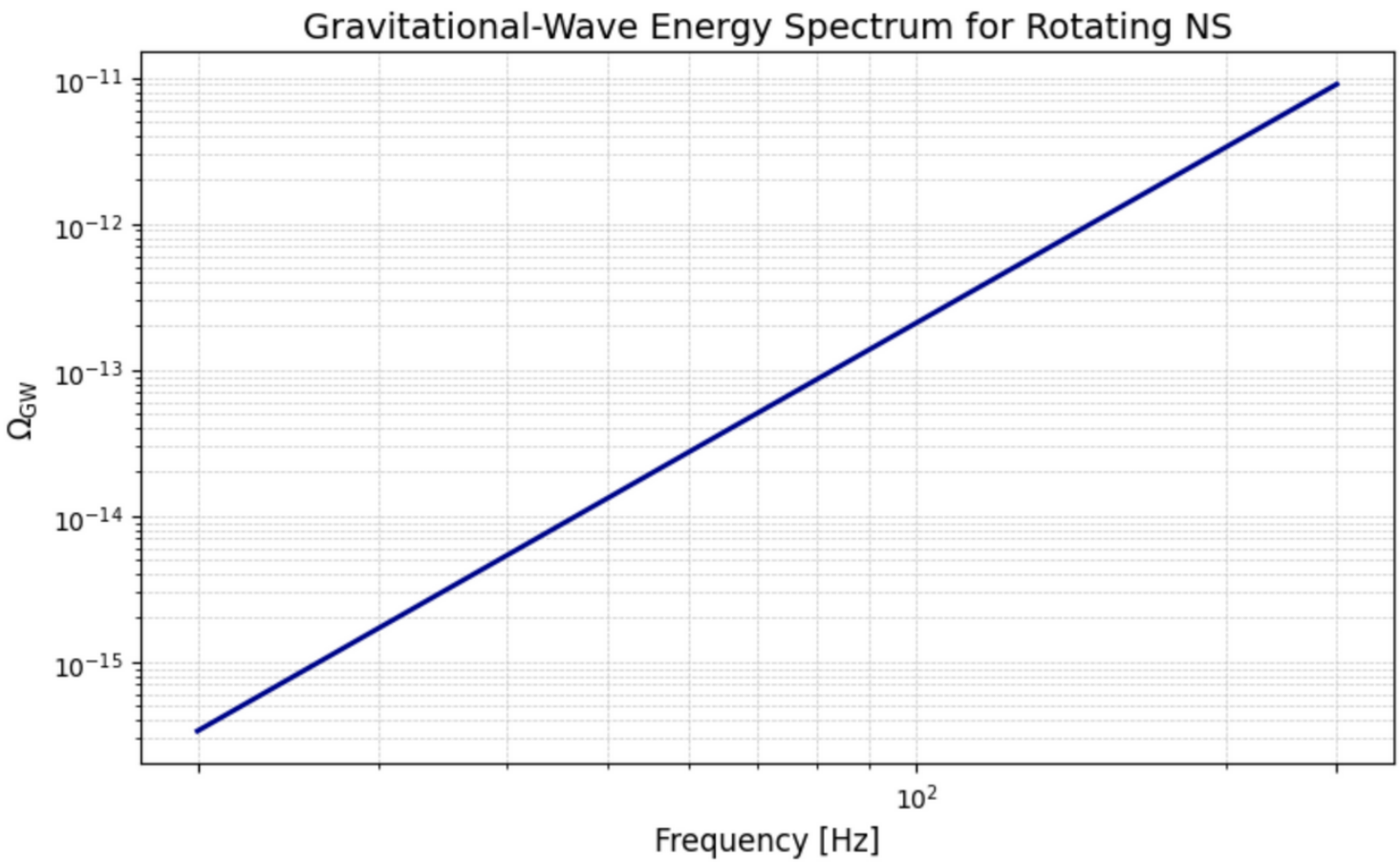

[4] K. Crocker et al., Phys. Rev. D., 95:063015, 2017

[5] E Howell et al., Class. Quant. Grv., 21:S551-S555, 2004

Magnetars

A magnetar is a type of NS with an extremely strong magnetic field ($\sim 10^{15}\,\mathrm{G}$).

- Detecting magnetars via GWs is challenging, as their electromagnetic emission typically dominates over GW emission.
- They are expected to constitute only about 10% of the total NS population contributing to the SGWB.

Yet, strong magnetic fields can induce significant deformations in the NS, increasing its ellipticity and enhancing GW emission to potentially detectable levels[6],[7].

The energy density spectrum follows the same general form as for rotating NSs, but with different expressions for the spectral energy $\frac{dE_{GW}}{df}$ and the event rate $\frac{dR(z)}{dz}$.

---

[6] T. Regimbau, V. Mandic, Class.Quant.Grav.25:184018,2008

[7] P. A. Rosado, Phys. Rev. D., 86:104007, 2012

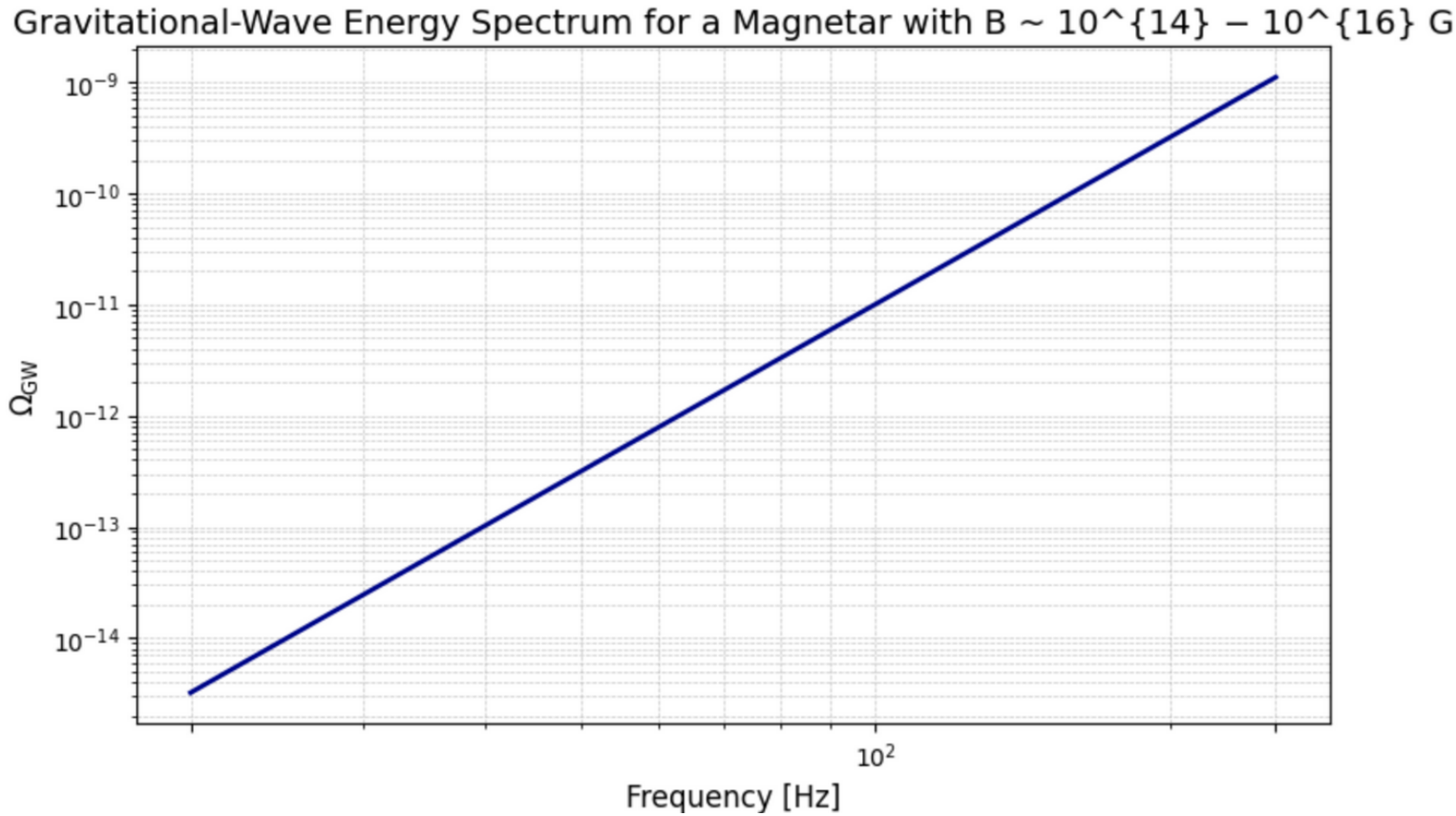

An example of the energy spectrum for a magnetar with $B \approx 10^{14} - 10^{15} G$.

NS Phase Transitions

Hadron–quark phase transitions:

- Occur in NS cores; quarks deconfine from hadrons.
- Micro-collapse due to softer quark EOS vs. stiffer hadronic EOS.
- Excites stellar oscillations, releasing gravitational waves.

Assumptions :

- ΛCDM cosmology
- Parameterized field theory with non-linear meson-baryon couplings
- Population II stars
- Initial mass function (IMF), minor effect on outcome

Energy density spectrum [8]:

$$\Omega_{GW}(f) = \frac{\pi f}{2\rho_c G} \int dz\, h_{NS}^2\, \dot{\rho}_*(z) \frac{dV}{dz}\, f_{pt} \int dm\, \phi(m)$$

[8] X.-J. Zhu et al., Gen. Rel. Grav., 41:1389, 2009

The Salpeter initial mass function is used and $\frac{dV}{dz}$ includes the proper distance and the comoving volume element as a function of redshift. The micro-collapse contribution is approximately:

$$h_{NS} \approx 10^{-19} \left(\frac{E}{M_\odot c^2} \right) \left(\frac{2\,\mathrm{kHz}}{f} \right)^{1/2} \left(\frac{\mathrm{Mpc}}{d_L} \right).$$

The star formation rate (SFR) $\dot{\rho}_*(z)$ follows the Springel & Hernquist model. [9]

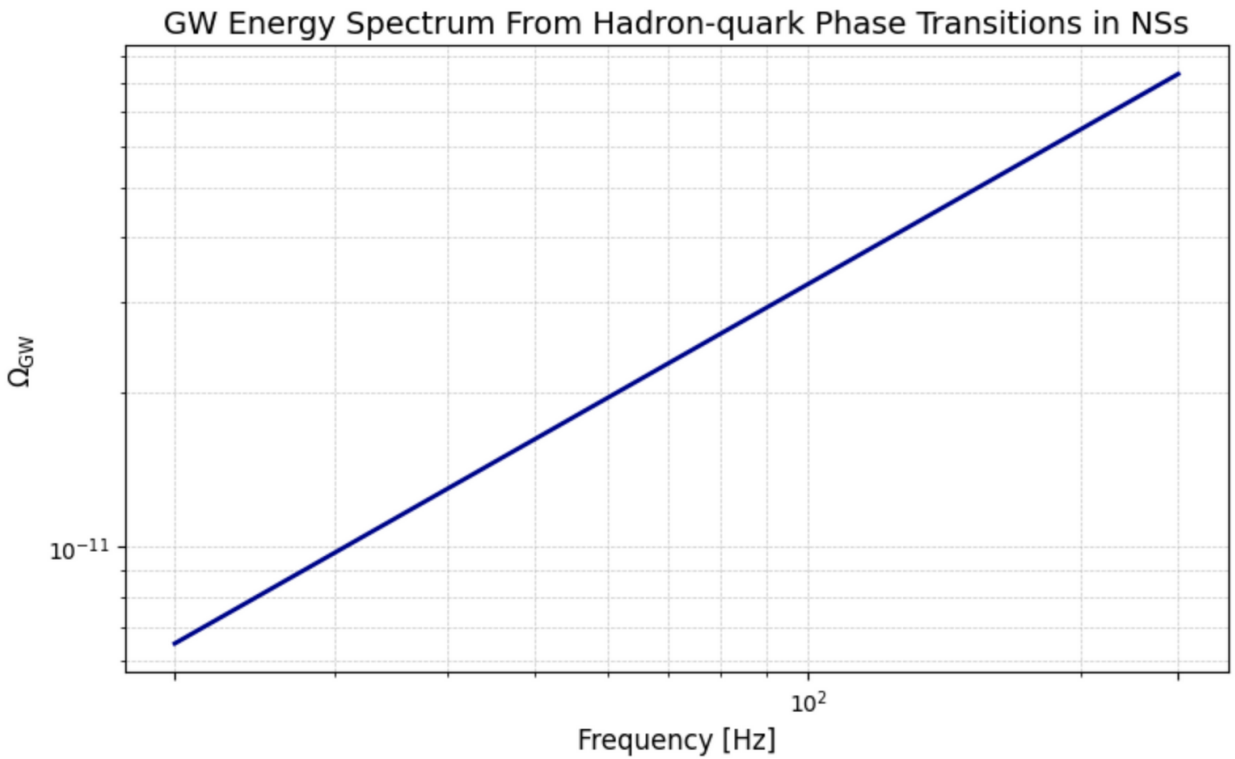

[9] X.-J. Zhu et al., Mon. Not. Roy. Astron. Soc., 431:882-899, 2013

Supernova Signals

A general expression for the energy spectrum from core-collapse supernovae (CCSNe) for redshift $z \lesssim 10$ follows the same form as for rotating neutron stars.

- The exact form of the functions within the integrand depends on the model.
- $R(z)$ depends on λ, the mass fraction converted into progenitors, and the SFR, along with Hubble parameter, similar to the terms used for NSs.
- Historically, most SFR estimates have been derived from luminosity measurements. Alternatively, gamma-ray burst (GRB) rates provide an independent set of constraints. A general form[10] incorporates GRB rates, luminosity-based estimates, and optical depth measurements from WMAP to model the SFR.

[10] K. Nagamine et al., Astrophys. J., 653:881-893, 2006

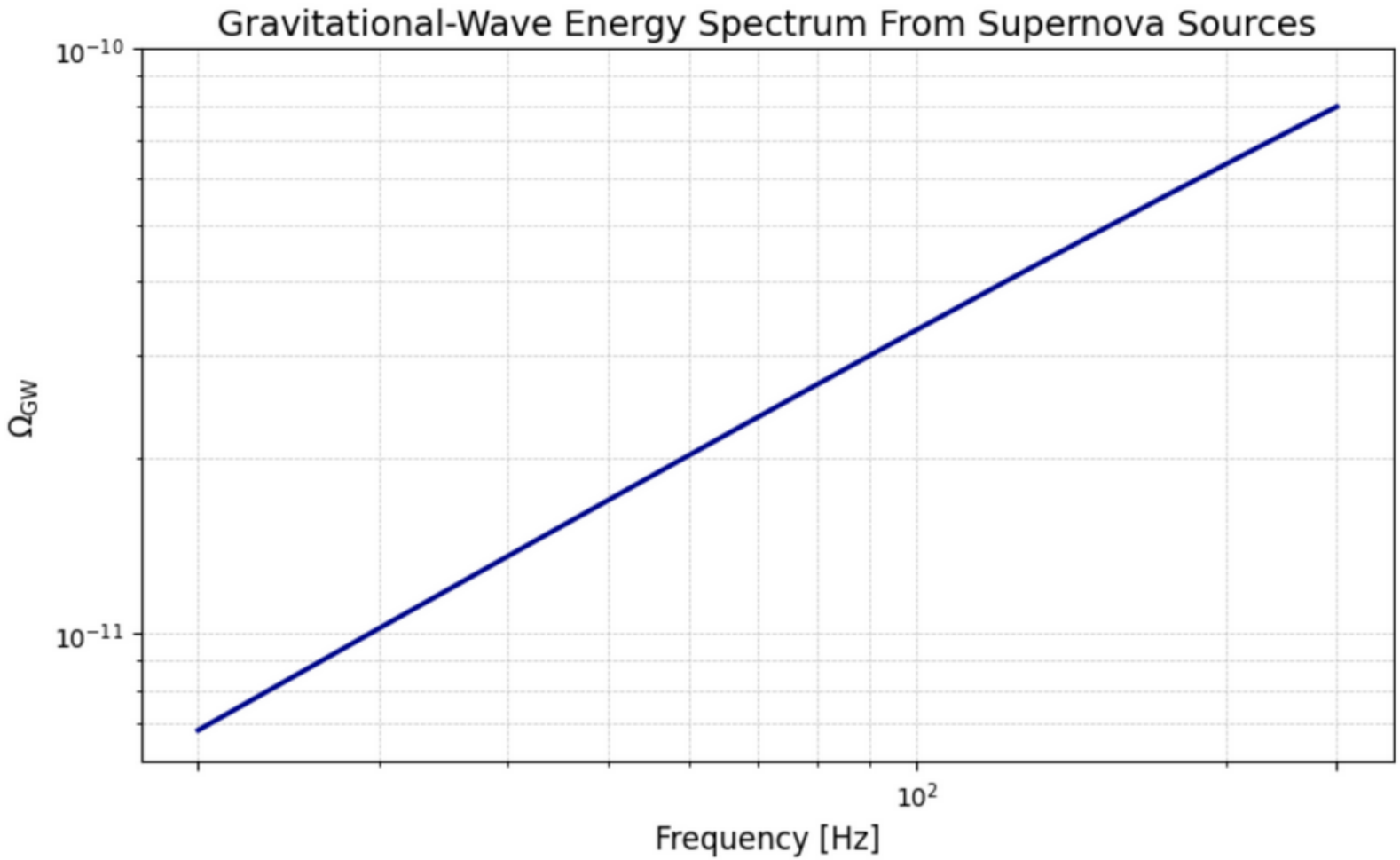

The energy spectrum is shown for $\lambda = 0.007 M_\odot$ and a Luminosity-based model for normal mode stars. A Gaussian spectrum is used as a suitable approximation.

The First Stars

Population III are first-generation stars.The form of the energy density spectra for the SGW is highly model dependent. One model has the following assumptions:

- A fully developed chemical evolution, the Daigne et al. (2006)
- ΛCDM cosmology.
- The Press-Schechter model of hierarchical structure formation
- Several bimodal star formation histories and also star formation from both the normal mode and the Population III mode.

$$\Omega_{GW}(f) = \frac{16\pi D^2}{15 G \rho_c} \int dz \frac{R(z) f_{source}^3 f |\tilde{h}(f_{source})|^2}{(1+z) H_o \sqrt{\Omega_\Lambda + (1+z)^3 \Omega_M}} \qquad (6)$$

- $R(z)$ is the cosmic supernova rate, and D is the distance to a typical SN.
- The GW spectrum shape $f|\tilde{h}(f)|$ depends on the total neutrino energy $E_\nu \sim 10^{53}\,\mathrm{erg}$ and the average anisotropy $\langle q \rangle$ from simulations ($\langle q \rangle = 0.45\%$)[11],[12].
- For a Population III progenitor of mass $300 M_\odot$ at $D = 10\,\mathrm{kpc}$, one finds:

$$f|\tilde{h}(f)| \simeq 2.6 \times 10^{-19} \left(1 + \frac{f}{0.2\,\mathrm{kHz}}\right)^3 \exp\left(-\frac{f}{0.3\,\mathrm{kHz}}\right).$$

[11] A. Buonanno et al., Phys. Rev. D., 72:084001, 2005

[12] E. Mueller et al., Astrophys. J., 603:221–230, 2004

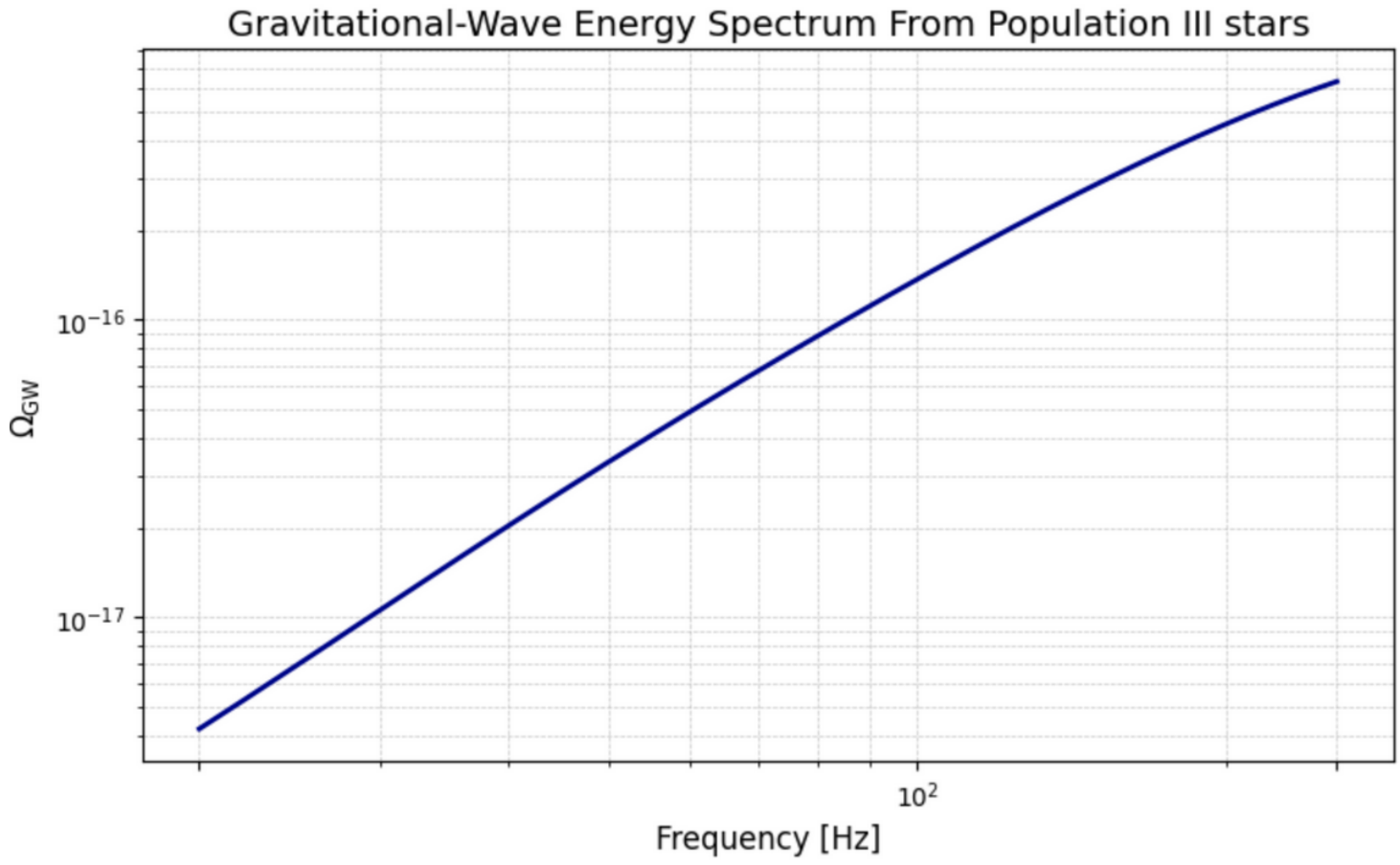
Gravitational-Wave Energy Spectrum From Population III stars
10^{-16}
10^{-17}
Ω_{GW}
10^{2}
Frequency [Hz]

Models with LIGO-scale GW Signatures

- **First-order cosmological phase transitions:** Strong electroweak phase transition (BSM Higgs sectors, singlets), Hidden/dark sector transitions (L. Velasco-Sevilla et al. 2412.17278), Inflation models (L. Velasco-Sevilla to appear) Grand Unified Models broken in several steps down to the SM (2506.07182)
- **Topological defects:** Cosmic strings (L. Velasco-Sevilla et al. 2112.14483), Domain wall collapse and annihilation
- **Primordial black holes (PBHs):** Formation from early-universe density fluctuations, PBH binaries and mergers
- **Exotic inflationary scenarios:** Preheating after inflation (parametric resonance), Spectator fields generating enhanced tensor modes
- **Axion-like and scalar fields:** Oscillons and scalar condensate fragmentation, Axion domain walls and string networks

For example, for first-order phase transitions we have the following spectral shape

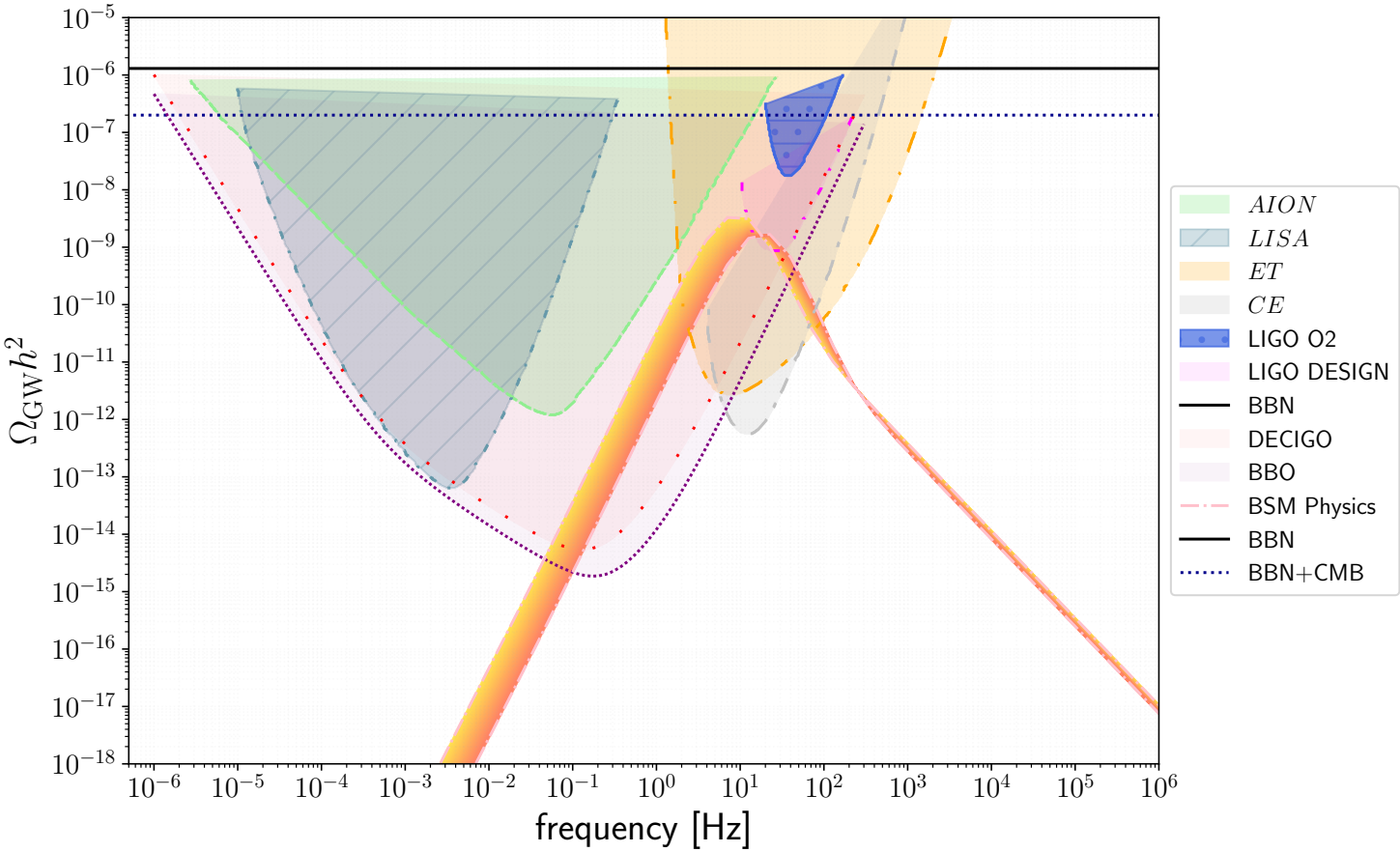

The goal is to disentangle these kinds of signals from those of astrophysical origin.

Summary and Outlook

- The detection of a stochastic cosmological signal entails the rigorous disentanglement of astrophysical foregrounds, thereby necessitating the development of a comprehensive and methodologically robust analysis framework.
- The development of advanced statistical methodologies is therefore indispensable for reliably disentangling signals of diverse origin and securing robust cosmological inference.
- A comprehensive analysis must account for all plausible astrophysical sources to enable robust comparison with cosmological signals.
- Apply parameter estimation using our extended model that includes both cosmological and astrophysical sources.
- Account for additional modeled contributions, e.g., detector noise sources.
- Future work: extend the analysis beyond LVK sensitivities to next-generation detectors.

Backup slides

From Advanced LIGO's and Advanced Virgo's Third Observing Run[13].

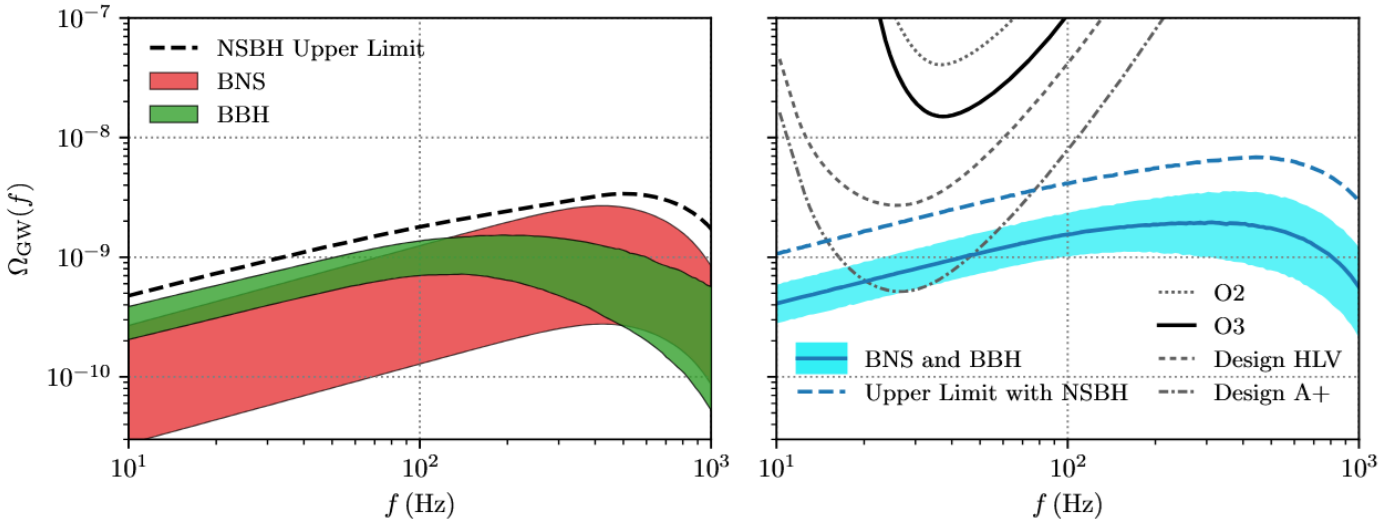

FIG. 5. Fiducial model predictions for the GWB from BBHs, BNSs, and NSBHs, along with current and projected sensitivity curves. In the left panel we show 90% credible bands for the GWB contributions from BNS and BBH mergers. Whereas the BNS uncertainty band illustrates purely the statistical uncertainties in the BNS merger rate, the BBH uncertainty band additionally includes systematic uncertainties in the binary mass distribution, as described in the main text. As no unambiguous NSBH detections have been made, we only show an upper limit on the possible contribution from such systems. The right panel compares the combined BBH and BNS energy density spectra, and 2σ power-law integrated (PI) curves for O2, O3, and projections for the HLV network at design sensitivity, and the A+ detectors. The solid blue line shows the median estimate of $\Omega_{\mathrm{BBH+BNS}}(f)$ as a function of frequency, while the shaded blue band illustrates 90% credible uncertainties. The dashed line, meanwhile, marks our projected upper limit on the total GWB, including our upper limit on the contribution from NSBH mergers.

[13] R. Abbot et al., Phys. Rev. D., 104:022004, 2021